Pressure effects on collective density fluctuations in water and protein solutions

Daniela Russo[a,b,1], Alessio Laloni[a], Alessandra Filabozzi[c], and Matthias Heyden[d,1]

[a]Istituto Officina dei Materiali, Consiglio Nazionale delle Ricerche, Institut Laue Langevin, 38042 Grenoble, France; [b]Institut Lumière Matière, Université de Lyon 1, 69622 Lyon, France; [c]Dipartimento di Fisica, Università di Roma Tor Vergata, I-00133 Rome, Italy; and [d]Theoretische Chemie, Max-Planck-Institut für Kohlenforschung, D-45470 Mülheim an der Ruhr, Germany

Edited by Sol M. Gruner, Cornell University, Ithaca, NY, and accepted by Editorial Board Member Pablo G. Debenedetti September 8, 2017 (received for review March 30, 2017)

Neutron Brillouin scattering and molecular dynamics simulations have been used to investigate protein hydration water density fluctuations as a function of pressure. Our results show significant differences between the pressure and density dependence of collective dynamics in bulk water and in concentrated protein solutions. Pressure-induced changes in the tetrahedral order of the water HB network have direct consequences for the high-frequency sound velocity and damping coefficients, which we find to be a sensitive probe for changes in the HB network structure as well as the wetting of biomolecular surfaces.

high pressure | hydration water | collective THz modes | molecular dynamics | neutron scattering

High-pressure effects on protein structure and dynamics are of significant interest in biology, not only to account for the adaptation of life to extreme environments but also to understand how macromolecules behave under normal conditions (1, 2). Pressure can modulate protein activity (3), and it may lead to dissociation of oligomeric proteins (4) and other supermolecular structures (5), induce (6) or inhibit (7, 8) the formation of aggregates and amyloid fibrils, induce denatured states (9), and modify their solvation (10). High pressure makes it possible to explore different conformational substates and to study folding and unfolding (11) and affects the kinetics of enzymatic reactions (9, 12). In some cases, high pressure increases the local roughness of the free energy landscape, thus increasing the depth of local minima and stabilizing intermediate states (13–15). A general feature of pressure-induced effects on protein dynamics is the slowing down of motions and a consequent stiffening and an increase of relaxation times (13–15).

Moderate, nondenaturing pressures induce an elastic response of solvated proteins. The applied pressure modifies the packing and order of the solvent at the protein surface, increases the protein hydration, and promotes the penetration of water in hydrophobic cavities (16, 17). This induces swelling and eventually unfolding at pressures sufficient for denaturation (18). Detailed changes in protein hydration at elevated pressures have been observed in molecular dynamics simulations of isolated proteins in solution, i.e., distortion of tetrahedral structure and stiffening of vibrational modes (19).

Detailed comparisons of pressure-induced effects (at moderate nondenaturing pressures $\lesssim$3 kbar) in protein solutions and the bulk solvent can provide insights into the hydration of proteins. Small-angle X-ray scattering (SAXS) and neutron scattering experiments have been recently combined by Russo and coworkers (20–22) to investigate high pressure-induced changes on particle–particle interactions, low-resolution structure, and global and local dynamics of lysozyme in aqueous solutions. The results showed that lysozyme maintains its globular structure up to at least 1,500 bar, while the density of the hydration shell slightly increases as a function of pressure. This causes a moderate nonlinear change in the effective protein–protein interaction potential observed by SAXS measurements (20, 23). At the same time, local dynamics described by mean square displacements of the protein protons [measured by quasi-elastic neutron scattering (QENS)] decreases as pressure increases, suggesting a loss in mobility following an increase of the hydration shell density. Both global and local protein dynamics change at the same threshold pressure, and for timescales accessible in a QENS experiment (ps), a transition from diffusive internal protein dynamics to localized motions within a local potential energy well has been observed (20, 21). This behavior has been attributed to denser structural packing of the first protein hydration layer at elevated pressure.

A similar behavior can be also found for other examples of biomolecular interfaces (24). However, we note that in protein hydration water pressure-induced disruption of the tetrahedral water structure can speed up local dynamics, such as translational and rotational diffusion and HB rearrangements (19, 25–28). In the context of the present study, it is important to note that collective and local single-particle dynamics describe fundamentally different processes. Single-particle dynamics as reported by QENS report on atomic mobilities of the nondeuterated fraction of a system, while coherent scattering experiments are sensitive to the propagation of density fluctuations in the entire system due to dynamic correlations in time and space.

To shed light on pressure effects on the structure of the protein hydration water hydrogen bond (HB) network and its correlation to a general slowdown of protein dynamics, we investigate here the collective dynamics of water in the presence of solvated proteins, combining coherent neutron scattering with computer simulations. Collective dynamics of water on an energy scale of 5–30 meV provide direct insights into correlated intermolecular vibrations (29, 30), i.e., propagating density fluctuations in the HB network of an aqueous solution. These modes are sensitive to HB network properties and therefore provide an excellent tool to study solute- and pressure-induced changes in water and aqueous solutions. Coherent scattering experiments and molecular dynamics simulations have therefore been used frequently to study collective dynamics in

Significance

This is a combined study, which employs neutron scattering experiments and molecular dynamics simulations to compare high pressure-induced effects on collective properties of protein solutions and bulk water, to observe changes in the HB network structure of protein hydration water upon compression. Our experimental results reflect distinct properties of water at the protein–water interface, while at the same time atomistic molecular dynamics simulations allow us to analyze its pressure-dependent structural changes. This study therefore provides insights that allow establishing measurements of pressure-induced variations in collective dynamics as a probe to characterize biomolecular systems as complex as entire cells.

Author contributions: D.R. and M.H. designed research; D.R., A.L., A.F., and M.H. performed research; D.R. and M.H. analyzed data; and D.R. and M.H. wrote the paper.

The authors declare no conflict of interest.

This article is a PNAS Direct Submission. S.M.G. is a guest editor invited by the Editorial Board.

[1]To whom correspondence may be addressed. Email: russo@ill.fr or heyden@kofo.mpg.de.

This article contains supporting information online at www.pnas.org/lookup/suppl/doi:10.1073/pnas.1705279114/-/DCSupplemental.

biomolecular solutions and even in living cells or the influence of temperature and/or pressure on the HB network of bulk water (30–37).

Methods

Here we study room temperature neutron Brillouin measurements of lysozyme solutions combined with molecular dynamics simulations as a function of pressure. The analysis of experimental results provides a description of dispersion curves, defining the active collective modes that propagate within the sample, and the damping factor, related to the propagation lifetimes. The measurements were performed on concentrated solutions of lysozyme (10% wt/wt) dissolved in D_2O buffer (10 mM Tris, pD = 6.0) using the time of flight neutron Brillouin spectrometer (BRISP) and a titanium alloy large-volume, high-pressure sample holder (see *SI Appendix* for experimental details). To obtain information on the protein interface and the contribution of the hydration water layer, both lysozyme solution and neat D_2O were measured at pressures of 1 bar, 2kbar, and 3 kbar. The stability of the protein solutions under the experimentally studied conditions has been established by pressure denaturation studies in the literature using various experimental probes, including Raman spectroscopy, NMR (38), and tryptophane fluorescence (39, 40) (see *SI Appendix* for more detailed discussion). Molecular dynamics simulations were carried out for bulk water and for solvated lysozyme proteins, in dilute and high-concentration conditions (10% wt/wt), at pressures of 1 bar, 500 bar, 1 kbar, 2 kbar, 3 kbar, and 5 kbar, allowing microscopic insights into structural changes in water and the protein hydration shell as a response to pressure (see *SI Appendix* for simulation details).

At the experimentally studied protein concentration, approximately two thirds of all water molecules are found at distances greater than 10 Å from the protein surface based on our simulation models, suggesting a significant amount of bulk-like water.

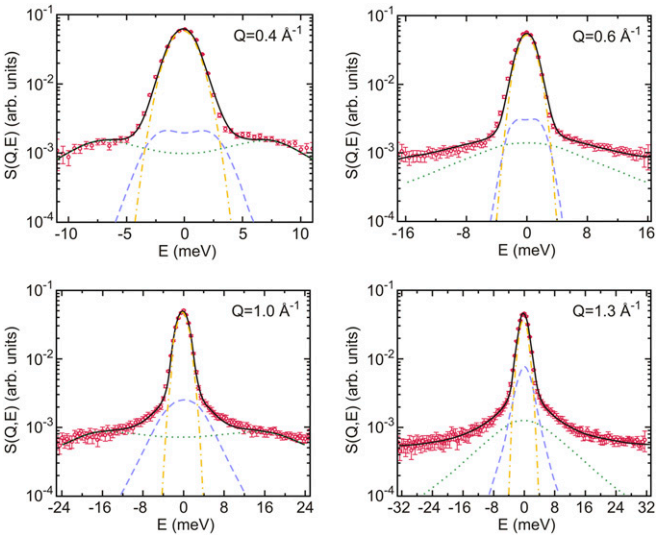

Fig. 1. Coherent inelastic spectra of lysozyme solution at 2 kbar at selected Q values. The thick black line shows fits of the two-component DHO model (see *SI Appendix* for details). The dashed blue and dotted green lines represent the resulting low- and high-frequency DHO, respectively. The dashed–dotted yellow line shows the experimental resolution function.

Results and Discussion

Fig. 1 shows experimental data at four selected wave vectors obtained for the lysozyme solution at 2 kbar, together with the best fit using a two-component damped harmonic oscillator model (DHO; see *SI Appendix* for details).

The dependence of the fitted DHO frequencies on the momentum transfer Q defines the dispersion curves shown in Fig. 2. Only the high-frequency mode is of dispersive nature and will be discussed in the following paragraphs. Fig. 2 shows a comparison of the experimental dispersion curves of lysozyme solution (Fig. 2*A*) and neat D_2O (Fig. 2*B*) as a function of pressure. Fig. 2*A* further shows a dispersion curve corresponding to measurements on *Escherichia coli* cells at ambient pressure from a previous study (32). The pronounced similarity to the concentrated protein solution at the same pressure shows that collective properties in both samples are comparable. Differences between collective dynamics in protein solutions, living cells, and bulk water at ambient pressure are statistically significant but small compared with pressure-induced changes. Considering high water concentrations of up to 80% within cells (41), this observation would be consistent with largely bulk-like collective properties of water within cells as probed via coherent neutron scattering. From the slope of the linear regime (between Q = 0.2 and 1.1 Å^{-1}), we obtain a propagation velocity of density fluctuations, i.e., the high frequency or fast sound velocity, of 3,460 ± 160 m/s for the collective excitation in the protein solution at ambient pressure. The corresponding slope of the dispersion curve for neat D_2O is equal to 3,040 ± 50 m/s. Both the pure water samples and the concentrated protein solutions show a statistically significant increase of the propagation velocity with increasing pressure. For the protein solution, the propagation velocity of the high-frequency mode increases to 3,730 ± 180 and 3,920 ± 210 m/s at 2 and 3 kbar, respectively. The corresponding propagation velocities in the neat water sample are observed as 3,530 ± 175 and 3,770 ± 188 m/s at 2 and 3 kbar.

The comparison between neat water and protein solutions allows us to study differences in pressure-induced changes of collective dynamics in both samples, which are attributed to the presence of the proteins and their interactions with the surrounding hydration water.

At equivalent pressures, the sound propagation velocity in the protein solution is higher compared to bulk water in the studied pressure range (*SI Appendix*, Fig. S2), suggesting an increased rigidity of the water HB network in the presence of the protein. This interpretation agrees with experimental observations and simulations that observe a slowdown of dynamical processes in the protein hydration shell. This applies, for example, to translational and rotational motions of water molecules as probed by magnetic relaxation dispersion (42), nuclear Overhauser effects in reverse micelles (43), Overhauser dynamic nuclear polarization (44), and ultrafast fluorescence (45, 46), to name but a few. Numerous molecular dynamics simulations reproduce these observations (47–50). The consensus is an up to twofold dynamical retardation for the majority of water molecules in a protein hydration shell, while only a small number of water molecules might be strongly bound and therefore further immobilized.

In our present study, we find that for both samples bulk water and the protein solution propagation velocities further increase with pressure. We note that the increase in the propagation velocity is not the result of an increased rigidity of the water HB network as one would define it based on noncollective, single-particle dynamics, for example, via lifetimes of individual HBs. The pressure-induced distortion of the water HB network structure weakens water–water HBs, hence decreasing the average lifetime (19, 25, 27, 28).

From previous simulations and experiments, it is known that the increase in pressure results in a slowdown of picosecond-timescale protein dynamics (14, 21), which might be intimately related to pressure-induced changes in the hydration environment. We highlight that the pressure dependence of the propagation velocity is more pronounced in bulk water than in the protein solution. Consequently, the difference in sound propagation velocities between both systems decreases at high pressure (linear extrapolation of the pressure-dependent experimental data yields equal sound propagation velocities in both systems at ∼4.4 kbar; see *SI Appendix*, Fig. S2 for details). Further, the sound propagation velocity in bulk water at 2 kbar (3,530 ± 175 m/s) is approximately equivalent to the sound propagation velocity in the protein solution at ambient pressure (3,460 ± 160 m/s). This indicates potential similarities of protein-induced and pressure-induced effects on the HB network structure of water, which largely determines the collective properties in both samples. An increased density of water in protein hydration shells, which would qualitatively mimic the effect of increased pressure, has been observed experimentally in combined X-ray and neutron scattering experiments (51).

For protein solutions, it has been shown that particularly the densities of the hydration layer are strongly pressure dependent (20, 21). In Fig. 3, we therefore analyze pressure-induced changes of the

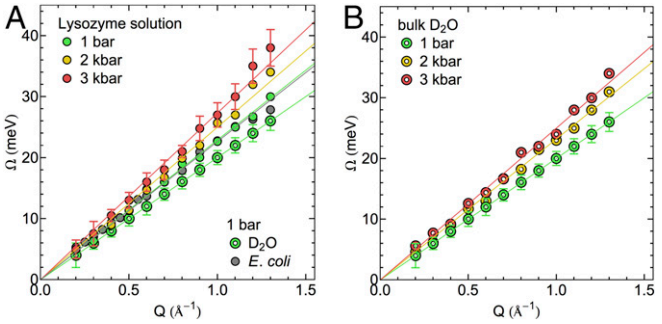

Fig. 2. Experimental dispersion curves of THz collective modes in hydration water of (*A*) lysozyme solution water network and (*B*) neat D_2O as a function of pressure (D_2O data for 1 bar from ref. 55). The dispersion curve of *E. coli* is reported in *A* for comparison (data from ref. 32). Error bars are equivalent for measurements at different pressures. For clarity, they are shown only for one respective data set for the protein solution and bulk water.

propagation velocity as a function of the sample density. Due to the lack of experimental densities for pressurized protein solutions, we obtained the density data from our molecular dynamics simulations of deuterated protein solutions and bulk D_2O. We also plot the sound velocity probed for water solvating hydrophilic and hydrophobic protein model interfaces at ambient pressure (52). Single-particle vibrations in these solutions at frequencies comparable to the ones studied here in the context of collective dynamics were previously shown to correlate with those of high-density amorphous (HDA) ice and low-density amorphous (LDA) ice, respectively (53). Therefore, we combined the sound velocities of both samples with the densities of HDA and LDA ice in Fig. 3, observing that they follow the overall observed trend. We note that the high-density data point (water solvating a hydrophilic surface) is found in close proximity to bulk D_2O at ~2 kbar. Interactions with the hydrophilic model interface at ambient pressure therefore also give rise to qualitatively similar changes in the water HB network as found for the protein solution; that is, they resemble densities and collective dynamics of pressurized water. The high-density region, represented in Fig. 3, shows an approximate linear density dependence of the sound velocity. The plotted data points provide a weak indication that this trend may not hold for densities lower than 1.1 g/cm^3. We note that Krisch et al. (54) observed an anomalous feature in X-ray scattering experiments of H_2O between 1.1 and 1.17 g/cm^3, i.e., a shoulder in the density-dependent sound velocity. The data shown in Fig. 3 exhibit a similar behavior; however, the small number of data points and the statistical error bars of the sound velocities inhibit a direct comparison. Arguably, the feature observed by Krisch et al. (54) might be expected at higher densities in our sample due to the use of D_2O in neutron scattering experiments. Krisch et al. (54) also show that the dependence of the low-frequency, hydrodynamic sound velocity on the increasingly distorted HB network structure for increasing pressure is more pronounced compared with the high-frequency sound velocity analyzed here. However, our results show that the high-frequency sound velocity is suitable to observe distinct pressure-induced changes in bulk water and protein hydration water due to differences in the structural response upon compression.

Further analysis of the related damping factors gives access to the lifetimes of the collective modes (see *SI Appendix* for details). Fig. 4 reports the damping factors of lysozyme solution (Fig. 4*A*) and neat D_2O (Fig. 4*B*) as a function of pressure. The results show underdamping ($0.5 < \Gamma/\Omega < 1$) for bulk water at ambient pressure over the entire Q range within the DHO model. We note that a constant damping ratio has been imposed in the underlying fit of this data set, which was obtained from ref. 55, while no such constraint has been used for the remaining datasets reported here. However, in pressurized D_2O this trend is unchanged in the low-Q range, and the damping ratio remains <1. At $Q > 1.0$ Å^{-1} a transition toward high, close-to-critical damping ratios occurs ($\Gamma/\Omega > 1$), which approaches critical damping ($\Gamma/\Omega = 2$) at pressures of 3 kbar. Within the simple DHO picture, this means that short-wavelength pressure fluctuations ($2\pi/Q$ on the order of intermolecular distances) in compressed water (2–3 kbar) decay in an increasingly nonoscillatory fashion with lifetimes on the same order of magnitude as the period of underlying intermolecular vibrations. Equivalently to the increase of propagation velocities, the increased dampening of short-wavelength fluctuations indicates pressure-induced structural changes in the HB network. In the concentrated protein solution, close-to-critical damping ($\Gamma/\Omega > 1$) of short-wavelength pressure fluctuations occurs already at ambient pressure. The ratio Γ/Ω at high Q values ($Q > 1.0$ Å^{-1}) experiences only a small change between 1 bar and 2 kbar. However, at 3 kbar the critically damped regime is reached, resulting in fast exponential decays of pressure fluctuations described by the fitted DHO model. We note that also in case of dampening of short-wavelength fluctuations, protein-induced effects at ambient pressure resemble the properties of bulk water at elevated pressure. In addition, with increasing pressure the differences between bulk water and the protein solutions in terms of short-wavelength dampening at $Q \sim 1.3$ Å^{-1} decrease, equivalently to increasingly similar propagation velocities. However, the onset of critical damping for the highest pressure remains a distinct characteristic feature of the protein solutions.

To investigate in more detail the structural changes in the water HB network with increasing pressure, we employ molecular dynamics simulations. First, we validate the simulation model by analyzing the pressure dependence of its collective properties as a function of pressure and compare it to the experimental observations. For this purpose, we utilize simulations of a deuterated multiprotein system resembling the experimental concentration of 10% wt/wt, which contains five lysozyme proteins, ~30,000 water molecules, and 40 chloride ions for charge neutralization (illustrated in Fig. 5*A*). A bulk D_2O simulation of approximately the same size is used as reference. The collective dynamics are analyzed directly via the longitudinal current spectrum $I^{\parallel}(Q,\omega)$ obtained from space–time Fourier transformations of density currents computed from atomic velocities (*SI Appendix*). The longitudinal current spectrum is related to the dynamic structure factor via $I^{\parallel}(Q, E=\hbar\omega) = (\omega^2/Q^2)S(Q,E)$. The propagation velocities of density fluctuations are obtained equivalently to the processing of the experimental data via (*i*) fitting of a two-component DHO model for $S(Q,E)$ and (*ii*) extracting the linear Q dependence of the dispersive high-frequency mode. We note that we limit the quantitative analysis to the determination of the frequency and propagation velocity of the dispersive high-frequency mode. As an example, the longitudinal current spectrum, the frequencies of the high-frequency mode obtained from the DHO fit, and the corresponding linear fit of its Q dependence are shown for the protein solution at a pressure of 2 kbar in Fig. 5*B*. Propagation velocities observed for bulk water, and the protein solutions are shown as a function of pressure and the corresponding density in

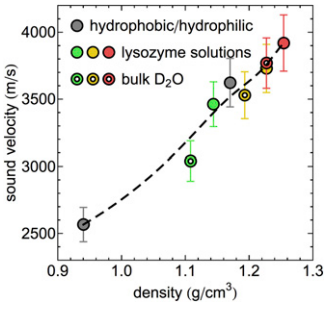

Fig. 3. Density dependence of the sound velocity of D_2O and lysozyme solution at various pressures. Data obtained for solutions containing large concentrations of hydrophilic and hydrophobic biointerface are shown according to ref. 52. Colors indicate the distinct pressures equivalent to Fig. 2. The dashed line serves as a guide to the eye.

Fig. 5 *C* and *D*, respectively. In qualitative agreement with the experimental results, we find increased propagation velocities in the protein solutions compared with bulk D_2O, when compared at equivalent pressures. When propagation velocities are compared as a function of the system density, the collective properties of bulk water and the protein solution describe essentially the same linear trend, which agrees with the experimental observations in the high-density regime in Fig. 3.

While we observe some quantitative differences between simulations and experiments, the qualitative trends observed experimentally for the pressure-dependent propagation velocity are reproduced. To analyze pressure-induced structural changes in the hydration water of the protein, we refer to a second set of simulations of a single solvated protein to simplify the analysis. Our structural analysis can be compared with previous work by Lerbret et al. (19). Our simulations show that the structure of the lysozyme protein is essentially constant within simulations on the 100-ns timescale for all pressures studied here, as indicated by root mean squared deviations of nonhydrogen protein atoms between 1.6 and 2.4 Å in Fig. 6*A*. This confirms previous observations in experimental studies up to 1.5 kbar (20, 21) and an analysis of the stability of secondary structure elements up to pressures of 6 kbar in simulations on a shorter 10-ns timescale (19). To analyze structural changes in the protein hydration shell in comparison with bulk water, we analyzed water within 5 Å from the protein surface as illustrated in Fig. 6*B*. This included an analysis of tetrahedral order parameters q (Fig. 6*C*), which yields 1 for a perfectly tetrahedral environment and 0 for an ideal gas (56) (*SI Appendix*). We note that distributions of the q parameter indicate two distinct subpopulations of water molecules: one with a relatively high tetrahedral order ($q = 0.8$) and one with a lower tetrahedral order ($q = 0.5$). Indications for both populations are observed for bulk water and protein hydration water. At ambient pressure the fraction of water molecules with low tetrahedral order is increased in protein hydration water compared to bulk water. With increasing pressure the population of water molecules with high tetrahedral order decreases, while the fraction of water molecules with low tetrahedral order increases. This is observed in the protein hydration shell and in bulk water. However, pressure-induced changes in the protein hydration shell are less pronounced compared with the bulk, resulting in increasingly similar distributions of the tetrahedral order parameter with increasing pressure. This is highlighted by the difference plot in Fig. 6*C*, *Bottom*. Consequently, we find that with increasing pressure differences between hydration shell water and bulk water structure become less pronounced. The pressure-induced structural changes in bulk water observed in our simulations reproduce previous work based on numerous empirical potentials (57). Likewise, the increased similarity of bulk and protein hydration water at high pressure in terms of the orientational order quantified by q seems to be independent of the underlying water model (19).

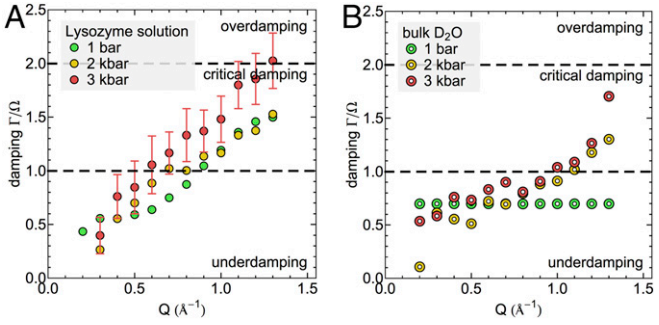

Fig. 4. Damping factors relative to mode frequency for (*A*) concentrated lysozyme solution and (*B*) neat D_2O with increasing pressure. The results for bulk water at 1 bar are reproduced from ref. 55. For clarity, error bars, equivalent for all measurements, are represented only for one dataset.

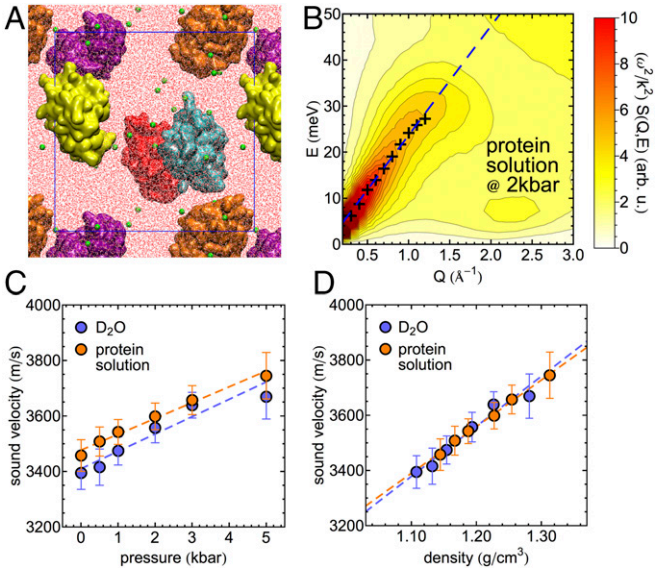

Fig. 5. Molecular dynamics simulations of concentrated protein solutions. (*A*) Snapshot of the simulated system containing five individual proteins (colored individually) in water (red and white) with chloride ions for charge neutralization (green spheres). The blue box indicates the periodically replicated simulation cell. (*B*) Simulated longitudinal current spectrum of the protein solution at 2 kbar. Crosses indicate the Q-dependent frequency of the high-frequency mode obtained from the fit between 0.3 and 1.2 Å^{-1}. The blue dashed line shows a linear fit of the mode position. (*C*) High-frequency sound velocity obtained from simulations of the protein solution and bulk D_2O as a function of pressure between 1 bar and 5 kbar. (*D*) Same as *C* shown as a function of the density observed in the respective simulation. Dashed lines in *C* and *D* indicate linear trends in the pressure- and density-dependent sound velocity data.

To understand this observation, we analyzed the structural changes in the protein hydration shell via density profiles measured as a function of distance from the protein surface (Fig. 6*D*). We compare our observations with radial distribution functions (rdfs) between water molecule centers of mass (COM) in bulk water simulations (Fig. 6*E*). With increasing pressure, we find a deformation of the first peak in the protein hydration water density profile. At ambient pressure the first peak between 2.5 and 4.0 Å is broad and shows indications of additional substructure, which we assign to the chemical heterogeneity of the protein surface, i.e., the distinct hydration of hydrophilic and hydrophobic groups. With increasing pressure, the peak narrows, and its intensity increases disproportionally compared with the accompanying increase in bulk water density. This indicates a more uniform hydration of the protein surface, independent of its chemical properties. Generally, this observation agrees with the pressure-induced increased hydration of hydrophobic pockets observed previously in T4-lysozyme mutants (17). A pressure-induced increase in the hydration of nonpolar atoms has also been observed in extensive simulations of the folding/unfolding equilibrium of the Trp-cage miniprotein, whereas the hydration of polar atoms was found insensitive to pressure (58). Changes in the relative hydration of polar and nonpolar surface groups quantified by solvent accessible surface areas at pressures of 3 kbar were also reported for simulations of apomyoglobin and lysozyme (59). In addition, Fig. 6*D* indicates an increased layering in the protein hydration shell, due to a more pronounced second peak, which increases in amplitude and changes its position from ∼6.5 Å at 1 bar to ∼6.0 Å at 5 kbar. Pressure-induced changes in the bulk water structure as described by the rdfs in Fig. 6*E* show qualitatively distinct characteristics, which are in accord with experimental data (60). The narrow first peak, describing the first shell of neighboring water molecules, is essentially unchanged with increasing pressure. Hence, the oxygen–oxygen

distance of water–water HBs is roughly pressure-independent. The structural response to increasing pressure mainly affects the first minimum and the second peak of the rdf, representing interstitial water and the second hydration shell, respectively. Both features are clearly resolved at ambient pressure. However, with increasing pressure water molecules from the second hydration shell penetrate into the interstitial region as a primary elastic response to compression, hence increasing the packing density (60, 61). The observations in Fig. 6 *D* and *E* explain the distinct behavior of the tetrahedral order parameters as a function of pressure in the protein environment and in pure water. In case of the protein hydration shell, the main elastic response to pressure-induced compression is the increased hydration of the protein surface, which requires a less pronounced change in the water HB network structure. In bulk water this predetermined breaking point is absent, and high pressures result in more pronounced changes in the tetrahedral HB network structure, mainly affecting HB angles and not HB lengths.

Generally, we recognize that the water structure and collective dynamics are distinct in the protein hydration shell and bulk water, which is reflected here by the difference in pressure-induced changes in collective dynamics. Our findings indicate that the tetrahedral order of the water HB network may be tightly linked to the high-frequency collective properties of water and protein solutions. Both experimentally observed propagation velocities and short wavelength damping coefficients are increased in protein solutions compared with bulk water of equivalent pressure, in qualitative agreement with the decreased tetrahedral order of the water HB network in the protein hydration shell. Likewise, differences between the collective properties of protein solutions and bulk water decrease with increasing pressure, akin to the increased similarity of the tetrahedral order parameter distributions in Fig. 6*C*. In experiments and simulations alike, the propagation velocities are roughly proportional to the total density of the system and seem relatively independent of the system composition

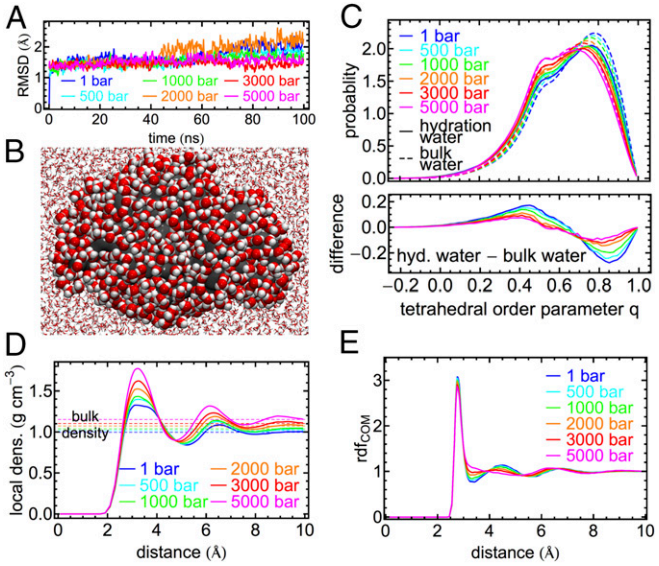

Fig. 6. Molecular dynamics simulations of solvated lysozyme protein and bulk water at pressures ranging from 1 bar to 5 kbar. (*A*) Root-mean-square deviation (RMSD) of all nonhydrogen atoms of the protein from the crystal structure in 100-ns simulations. (*B*) Snapshot from the simulation of a single lysozyme molecule (gray) illustrating water molecules within 5 Å of the protein (1 bar). (*C*) Distribution of the tetrahedral order parameter *q* in bulk water (dashed lines) and protein hydration water (solid lines; defined as water within 5 Å of the closest nonhydrogen protein atom). (*D*) Water density profiles measured as a function of distance to the protein surface (defined by distance to closest nonhydrogen protein atom). (*E*) Radial distribution functions (rdf) of water molecule centers of mass (COM) in bulk water.

(Figs. 3 and 5*D*). Protein solutions at ambient pressure, with an increased overall density and a protein-induced decrease of the tetrahedral order in the water HB network, exhibit collective dynamics that can be qualitatively compared with bulk water at increased pressures with an equivalent overall density. With increasing pressure, the overall densities and fast sound propagation velocities become increasingly similar between protein solutions and pure water, due to distinct pressure-induced changes in the water HB network structure.

However, we also note a qualitative difference in the pressure response of collective properties with and without solvated proteins. The onset of high dampening coefficients Γ, i.e., the occurrence of damping ratios $\Gamma/\Omega > 1$ at intermediate wavelengths, i.e., $Q < 1.0$ Å^{-1} (Fig. 4*A*), indicating increasingly nonoscillatory dynamics, is only observed for the protein solutions and occurs simultaneously with an increased hydration of the protein surface (Fig. 6*D*). Likewise, the damping of short-wavelength fluctuations ($Q > 1.0$ Å^{-1}) remains significantly more pronounced in protein solutions compared with bulk water, also at high pressures or equivalent densities. While it is difficult to provide a detailed microscopic interpretation of the damping of collective modes obtained in the fit of the DHO model, we recall the occurrence of a slowdown of protein dynamics as a response to increased pressure (20). Pressure induces an increase in hydration of the protein surface and therefore results in altered properties of the average protein–water interface in the solution. We may speculate that the observation of enhanced damping of collective modes in protein solutions and a slowdown of protein dynamics are related to each other because the dynamics of system components are coupled via the altered protein–water interface. Interactions between the protein and water at the biomolecular interface play an important role for the coupling of vibrational modes between both components. In previous simulations of hydrated protein crystals, it could be shown that collective modes, characteristic of the protein, propagate into the surrounding hydration water (62). Likewise, correlated protein–water vibrations and resulting collective modes were shown to depend on the chemical properties of the protein–water interface (63, 64).

Promising future extensions or our studies involve simultaneous variations in temperature and pressure. Raman spectroscopy studies of lysozyme solutions suggest that increased, nondenaturating pressures are able to reverse structural changes involved in early stages of thermal denaturation (65). Such pressure-induced suppressions of conformational fluctuations are likely to also affect picosecond-timescale, collective dynamics in the protein and its dynamical coupling to the surrounding water HB network.

Conclusion

In summary, this study investigates the pressure dependence of structural properties and collective dynamics in water and protein solutions for moderate, nondenaturing pressures between 1 bar and 3 kbar (up to 5 kbar in simulations). We find that protein hydration water exhibits some features of pressurized water and that with increasing pressure and density, differences in the water HB network structure and collective dynamics decrease, apart from critical damping of collective modes, which only occurs in protein solutions.

Previous experimental studies have shown that high-frequency sound propagation velocities between various biomolecular systems (protein or peptide solutions, living cells) are roughly comparable at ambient pressures, while fitted damping factors of the collective modes often exhibit distinct Q-dependent behavior (52). Here we add external pressure as an additional variable and observe distinct pressure-induced changes of high-frequency sound velocities and damping factors in absence or presence of solvated proteins. However, the overall density seems to remain the main factor influencing collective mode propagation on the experimental timescale, while the specific interactions between the solvated protein surface and the hydration shell, as well as the collective properties of the proteins themselves, seem to affect the damping.

In total, we find that pressure-induced changes of collective dynamics provide a promising probe to study the hydration of

biomolecules, providing information also relevant for ambient conditions, i.e., via the pressure-dependent hydration of the heterogeneous protein surface. Ambient pressure collective dynamics of various biological samples are currently an active field of research. In this context, it is essential to be able to provide microscopic interpretations for the available experimental observables, such as sound propagation velocities and damping. This combined experimental and theoretical study provides a crucial step along those lines because the pressure dependence allows us to analyze the influence of structural changes in the water HB network, either due to interaction with a solvated biomolecule or pressure, on the experimentally accessible properties.

ACKNOWLEDGMENTS. We thank A. De Francesco for his assistance during the experiment on the BRISP instrument and F. Formisano for providing the instrument data reduction routines. A.L. thanks S. Aisa from Dipartimento di Fisica, Università di Perugia, for his help in the high-pressure cell manufacture. D.R. thanks F. Sacchetti from Dipartimento di Fisica, Università di Perugia, for the financial support in the High-Pressure Cell project. This work is supported by the Cluster of Excellence RESOLV (Award EXC 1069) funded by the Deutsche Forschungsgemeinschaft (M.H.).

1. Luong TQ, Kapoor S, Winter R (2015) Pressure—A gateway to fundamental insights into protein solvation, dynamics, and function. *ChemPhysChem* 16:3555–3571.
2. Meersman F, McMillan PF (2014) High hydrostatic pressure: A probing tool and a necessary parameter in biophysical chemistry. *Chem Commun (Camb)* 50:766–775.
3. Makarov AA, et al. (2016) Use of hydrostatic pressure for modulation of protein chemical modification and enzymatic selectivity. *Org Biomol Chem* 14:4448–4455.
4. Silva JL, Weber G (1993) Pressure stability of proteins. *Annu Rev Phys Chem* 44:89–113.
5. Gebhardt R, Takeda N, Kulozik U, Doster W (2011) Structure and stabilizing interactions of casein micelles probed by high-pressure light scattering and FTIR. *J Phys Chem B* 115:2349–2359.
6. Jansen R, Grudzielanek S, Dzwolak W, Winter R (2004) High pressure promotes circularly shaped insulin amyloid. *J Mol Biol* 338:203–206.
7. Dzwolak W, Ravindra R, Lendermann J, Winter R (2003) Aggregation of bovine insulin probed by DSC/PPC calorimetry and FTIR spectroscopy. *Biochemistry* 42:11347–11355.
8. St John RJ, Carpenter JF, Randolph TW (1999) High pressure fosters protein refolding from aggregates at high concentrations. *Proc Natl Acad Sci USA* 96:13029–13033.
9. Mozhaev VV, Heremans K, Frank J, Masson P, Balny C (1996) High pressure effects on protein structure and function. *Proteins* 24:81–91.
10. Roche J, et al. (2012) Cavities determine the pressure unfolding of proteins. *Proc Natl Acad Sci USA* 109:6945–6950.
11. Silva JL, Foguel D, Royer CA (2001) Pressure provides new insights into protein folding, dynamics and structure. *Trends Biochem Sci* 26:612–618.
12. Real HJV, Alfaia AJ, Calado ART, Ribeiro MHL (2007) High pressure-temperature effects on enzymatic activity: Naringin bioconversion. *Food Chem* 102:565–570.
13. Erlkamp M, et al. (2015) Influence of pressure and crowding on the sub-nanosecond dynamics of globular proteins. *J Phys Chem B* 119:4842–4848.
14. Calandrini V, et al. (2008) Relaxation dynamics of lysozyme in solution under pressure: Combining molecular dynamics simulations and quasielastic neutron scattering. *Chem Phys* 345:289–297.
15. Appavou MS, Gibrat G, Bellissent-Funel MC (2006) Influence of pressure on structure and dynamics of bovine pancreatic trypsin inhibitor (BPTI): Small angle and quasi-elastic neutron scattering studies. *Biochim Biophys Acta* 1764:414–423.
16. Hummer G, Garde S, García AE, Paulaitis ME, Pratt LR (1998) The pressure dependence of hydrophobic interactions is consistent with the observed pressure denaturation of proteins. *Proc Natl Acad Sci USA* 95:1552–1555.
17. Collins MD, Hummer G, Quillin ML, Matthews BW, Gruner SM (2005) Cooperative water filling of a nonpolar protein cavity observed by high-pressure crystallography and simulation. *Proc Natl Acad Sci USA* 102:16668–16671.
18. Foglia F, et al. (2016) Water dynamics in Shewanella oneidensis at ambient and high pressure using quasi-elastic neutron scattering. *Sci Rep* 6:18862.
19. Lerbret A, Hédoux A, Annighöfer B, Bellissent-Funel MC (2013) Influence of pressure on the low-frequency vibrational modes of lysozyme and water: A complementary inelastic neutron scattering and molecular dynamics simulation study. *Proteins* 81:326–340.
20. Ortore MG, et al. (2009) Combining structure and dynamics: Non-denaturing high-pressure effect on lysozyme in solution. *J R Soc Interface* 6(Suppl 5):S619–S634.
21. Russo D, et al. (2013) The impact of high hydrostatic pressure on structure and dynamics of β-lactoglobulin. *Biochim Biophys Acta* 1830:4974–4980.
22. Filabozzi A, et al. (2010) Elastic incoherent neutron scattering as a probe of high pressure induced changes in protein flexibility. *Biochim Biophys Acta* 1804:63–67.
23. Schroer MA, et al. (2011) Nonlinear pressure dependence of the interaction potential of dense protein solutions. *Phys Rev Lett* 106:178102.
24. Russo D, et al. (2013) Evidence of dynamical constraints imposed by water organization around a bio-hydrophobic interface. *J Phys Chem B* 117:2829–2836.
25. Woolf LA (1975) Tracer diffusion of tritiated-water (Tho) in ordinary water (H_2O) under pressure. *J Chem Soc Faraday Trans 1* 71:784–796.
26. Jonas J, DeFries T, Wilbur DJ (1976) Molecular motions in compressed liquid water. *J Chem Phys* 65:582–588.
27. Bagchi K, Balasubramanian S, Klein ML (1997) The effects of pressure on structural and dynamical properties of associated liquids: Molecular dynamics calculations for the extended simple point charge model of water. *J Chem Phys* 107:8561–8567.
28. Smolin N, Winter R (2008) Effect of temperature, pressure, and cosolvents on structural and dynamic properties of the hydration shell of SNase: A molecular dynamics computer simulation study. *J Phys Chem B* 112:997–1006.
29. Rahman A, Stilling FH (1974) Propagation of sound in water—Molecular-dynamics study. *Phys Rev A* 10:368–378.
30. Tarek M, Tobias DJ (2002) Single-particle and collective dynamics of protein hydration water: A molecular dynamics study. *Phys Rev Lett* 89:275501.
31. Russo D, et al. (2016) Water collective dynamics in whole photosynthetic green algae as affected by protein single mutation. *J Phys Chem Lett* 7:2429–2433.
32. Sebastiani F, et al. (2013) Collective THz dynamics in living Escherichia coli cells. *Chem Phys* 424:84–88.
33. Bellissent-Funel MC, et al. (1989) Low-frequency collective modes in dry and hydrated proteins. *Biophys J* 56:713–716.
34. Rheinstädter MC, Ollinger C, Fragneto G, Demmel F, Salditt T (2004) Collective dynamics of lipid membranes studied by inelastic neutron scattering. *Phys Rev Lett* 93:108107.
35. Wang Z, et al. (2014) One role of hydration water in proteins: Key to the "softening" of short time intraprotein collective vibrations of a specific length scale. *Soft Matter* 10:4298–4303.
36. Yoshida K, Baron AQR, Uchiyama H, Tsutsui S, Yamaguchi T (2016) Structure and collective dynamics of hydrated anti-freeze protein type III from 180 K to 298 K by X-ray diffraction and inelastic X-ray scattering. *J Chem Phys* 144:134505.
37. Amann-Winkel K, et al. (2016) X-ray and neutron scattering of water. *Chem Rev* 116: 7570–7589.
38. Samarasinghe SD, Campbell DM, Jonas A, Jonas J (1992) High-resolution NMR study of the pressure-induced unfolding of lysozyme. *Biochemistry* 31:7773–7778.
39. Li TM, Hook JW, 3rd, Drickamer HG, Weber G (1976) Plurality of pressure-denatured forms in chymotrypsinogen and lysozyme. *Biochemistry* 15:5571–5580.
40. Chryssomallis GS, Torgerson PM, Drickamer HG, Weber G (1981) Effect of hydrostatic pressure on lysozyme and chymotrypsinogen detected by fluorescence polarization. *Biochemistry* 20:3955–3959.
41. Orecchini A, et al. (2012) Collective dynamics of intracellular water in living cells. *J Phys Conf Ser* 340:012091.
42. Halle B (2004) Protein hydration dynamics in solution: A critical survey. *Philos Trans R Soc Lond B Biol Sci* 359:1207–1223, discussion 1223–1224, 1323–1328.
43. Nucci NV, Pometun MS, Wand AJ (2011) Mapping the hydration dynamics of ubiquitin. *J Am Chem Soc* 133:12326–12329.
44. Cheng CY, Varkey J, Ambroso MR, Langen R, Han S (2013) Hydration dynamics as an intrinsic ruler for refining protein structure at lipid membrane interfaces. *Proc Natl Acad Sci USA* 110:16838–16843.
45. Pal SK, Peon J, Bagchi B, Zewail AH (2002) Biological water: Femtosecond dynamics of macromolecular hydration. *J Phys Chem B* 106:12376–12395.
46. Li T, Hassanali AAP, Kao YT, Zhong D, Singer SJ (2007) Hydration dynamics and time scales of coupled water-protein fluctuations. *J Am Chem Soc* 129:3376–3382.
47. Bagchi B (2005) Water dynamics in the hydration layer around proteins and micelles. *Chem Rev* 105:3197–3219.
48. Pizzitutti F, Marchi M, Sterpone F, Rossky PJ (2007) How protein surfaces induce anomalous dynamics of hydration water. *J Phys Chem B* 111:7584–7590.
49. Heyden M, Havenith M (2010) Combining THz spectroscopy and MD simulations to study protein-hydration coupling. *Methods* 52:74–83.
50. Bizzarri AR, Cannistraro S (2002) Molecular dynamics of water at the protein-solvent interface. *J Phys Chem B* 106:6617–6633.
51. Svergun DI, et al. (1998) Protein hydration in solution: Experimental observation by x-ray and neutron scattering. *Proc Natl Acad Sci USA* 95:2267–2272.
52. Russo D, et al. (2012) Brillouin neutron spectroscopy as a probe to investigate collective density fluctuations in biomolecules hydration water. *Spectrosc Int J* 27:293–305.
53. Russo D, et al. (2011) Vibrational density of states of hydration water at biomolecular sites: Hydrophobicity promotes low density amorphous ice behavior. *J Am Chem Soc* 133:4882–4888.
54. Krisch M, et al. (2002) Pressure evolution of the high-frequency sound velocity in liquid water. *Phys Rev Lett* 89:125502.
55. Sacchetti F, Suck JB, Petrillo C, Dorner B (2004) Brillouin neutron scattering in heavy water: Evidence for two-mode collective dynamics. *Phys Rev E Stat Nonlin Soft Matter Phys* 69:061203.
56. Errington JR, Debenedetti PG (2001) Relationship between structural order and the anomalies of liquid water. *Nature* 409:318–321.
57. Yan Z, et al. (2007) Structure of the first- and second-neighbor shells of simulated water: Quantitative relation to translational and orientational order. *Phys Rev E Stat Nonlin Soft Matter Phys* 76:051201.
58. Paschek D, Hempel S, García AE (2008) Computing the stability diagram of the Trp-cage miniprotein. *Proc Natl Acad Sci USA* 105:17754–17759.
59. Grigera JR, McCarthy AN (2010) The behavior of the hydrophobic effect under pressure and protein denaturation. *Biophys J* 98:1626–1631.
60. Soper AK (2000) The radial distribution functions of water and ice from 220 to 673 K and at pressures up to 400 MPa. *Chem Phys* 258:121–137.
61. Wroblowski B, Díaz JF, Heremans K, Engelborghs Y (1996) Molecular mechanisms of pressure induced conformational changes in BPTI. *Proteins* 25:446–455.
62. Conti Nibali V, D'Angelo G, Paciaroni A, Tobias DJ, Tarek M (2014) On the coupling between the collective dynamics of proteins and their hydration water. *J Phys Chem Lett* 5:1181–1186.
63. Heyden M, Tobias DJ (2013) Spatial dependence of protein-water collective hydrogen-bond dynamics. *Phys Rev Lett* 111:218101.
64. Heyden M (2014) Resolving anisotropic distributions of correlated vibrational motion in protein hydration water. *J Chem Phys* 141:22D509.
65. Remmele RL, Jr, McMillan P, Bieber A (1990) Raman spectroscopic studies of hen egg-white lysozyme at high temperatures and pressures. *J Protein Chem* 9:475–486.